New Methods to Model and Simulate Both Air Exchange and Particle Contamination of Portable Devices

Markus Olin[1], Lauri Laakso[2], Jukka Hannula[3], Timo Galkin[4], Kyösti Väkeväinen[5], Kari Hartikainen[6] and Eini Puhakka[1]
[1] VTT Technical Research Centre of Finland,
[2] University of Helsinki, Department of Physical Sciences, [3] Nokia Corporation
[4] Nokia Siemens Networks, [5] Metso Automation, [6] Ambertec Ltd
Finland

1. Introduction

Developed countries have made great efforts to improve air quality through adopting clean air plans, which have included measures such as demanding emission and air quality regulations, continuous air quality monitoring in urban/industrial centres and use of cleaner fuels such as natural gas. Meanwhile, in developing countries there is a clear phenomenon of migration from the countryside to the city, which has brought with it greater emissions into the atmosphere, mainly produced by biofuels used in cooking and heating and increasing traffic (Scholorling, 2000; Laakso et al., 2006) with the additional difficulty that in these countries the tendency is to have a stock of old, badly maintained vehicles. These factors have produced far-reaching changes in air quality in urban contexts, especially in the 1990s, when the majority of clean air plans were tightened up (Baldasano et al., 2003).
At the same time, markets for mobile devices have grown strongly in areas with high particle and pollutant concentrations (e.g., Asia, Africa and South America). Exposure to a high amount of fine particles, and the resulting contamination and corrosion, is a potential future reliability risk. To avoid this risk, one must understand the basic physics of particle drifting and, in addition, know the chemical and physical properties of the atmospheric aerosol particles. This includes the mapping and investigation of atmospheric measurements.
Telecommunication equipment is exposed to various kinds of stresses in the course of its life (Roberge et al., 2002; Hannula 2001; Ojala & Väkeväinen 2001; Väkeväinen et al., 2001). The stresses can be divided into mechanical, chemical, thermal, electrical and radiation stresses. The transport of potentially harmful chemical substances, partly or totally bound to fine particles, takes place via molecular diffusion and advection by air flow. Both direct measurements and simulation of flow velocities in electronic devices are complicated tasks, because of the detailed and heterogeneous structure of these devices. In addition to complex

structure, the effect of heat-producing components has to be taken into account since they may alter both the flow velocity and the structure of the device.
The main objectives of the study were to understand the basic chemistry and physics of

- fine particles, air pollution penetration and
- drifting of coarse particles (dust/sand)

into mobile device electronics (e.g., speakers, RF shields and metal display structures, which are the most sensitive to air pollution). Special attention was directed to so-called accumulation-range particles (80 to 1000 nm in diameter) because they are assumed to penetrate constructions such as mobile phones easily and their mass and reactive surface area is relatively large when compared to smaller particles.
Based on this information, the key aims were:

1. Understanding of particle drifts in miniature structures as phenomena.
2. Estimated particle size and number/mass distributions in various use environments.
3. A report concerning particle drifting and deposition in selected mobile devices, including estimation of good and possibly bad material and structural solutions.
4. A verified estimation model for particle drifting in miniature structures capable of estimating dependency on structural differences and particle sizes.
5. Establishment of the link between test conditions and real usage conditions, by using simulation methods.

Our approach has included several steps (see Fig. 1):

1. Development of a model for transport in air both inside and outside the equipment.
2. Development of a model for contamination processes – most often small particles in our cases.
3. Combining and simplification of this knowledge to create a contamination model able to predict phone contamination in a real user environment throughout the phone's service life.

Each step includes several smaller tasks (see Fig. 1). For example, study of air exchange was carried out in separate steps. First, gas flows in the mobile phone were investigated via the helium-based leakage method (its first application to electronic devices), and we observed that the results had no real meaning without extensive modelling. Next, these results were fitted by analytical models, incapable of any predictive calculations, to approximate diffusivity and permeability inside the phone. After that, a much more complicated numerical model was developed. A commercial tool, FEMLAB®, was applied to both apply realistic geometric structures and link several physical phenomena: transport of mass, heat and momentum. Finally, the numerical model was modified for cases where temperature differences (due to the heat-producing components) drive the gas transport. These four steps enabled calculation of air exchange coefficient values for a specific mobile phone model, for a typical use situation: phone on and vertically oriented.
The deposition of harmful aerosol particles in a mobile phone was approached with a similar multi-step approach: Deposition of different-sized particles was estimated via a combination of analytical and numerical approaches. For this, a coupled particle convection/diffusion and flow velocity model was developed to estimate deposition coefficients. First, equations for the flow velocity calculations and aerosol particle transport were formed. Second, the equations were implemented in FEMLAB® with Chemical Engineering Module. Finally, the model was applied in calculating important parameter values needed in the simplified contamination model.

Data from these two steps, gas exchange and deposition, could then be combined with experimental field data, phone user characteristics and an indoor air model modified to be suitable for the conditions inside a phone.

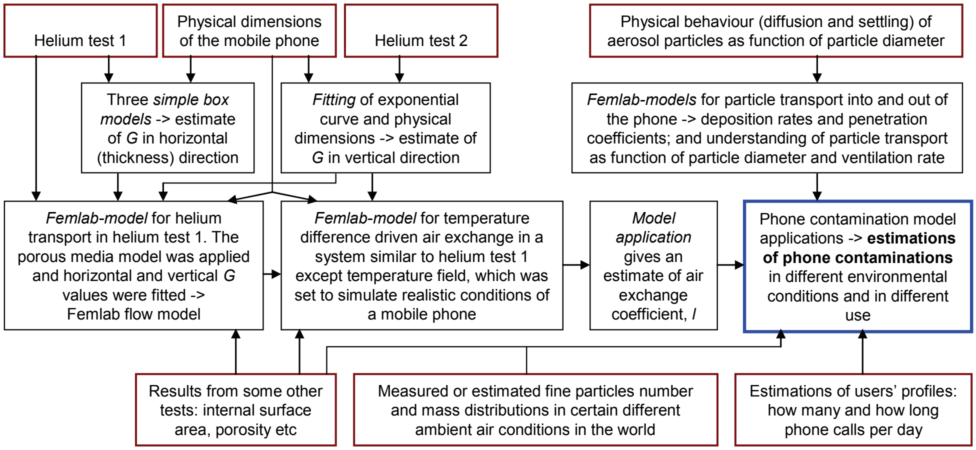

Figure 1. A schematic picture of the models and input parameters used in this study

2. Aerosol particles as a contaminating substance

Contamination of mobile devices may be caused by chemical compounds either in gas phase or bound to particles; water, either vapour or aqueous, is a very important contaminant and is discussed separately below.

2.1 Effect of chemical composition

Contamination caused by chemical compounds is one of the stresses detected in the structures of small electronic devices. The transport of chemical compounds is caused by molecular diffusion and advection by air flow. Chemical contamination is a very complex and unwanted phenomenon, which causes deposition formation on the surfaces of devices. Despite measurements, control and simulation of flow velocities in electronic devices, the problem of contamination still remains among the unsolved problems. Contamination leads to reduced functionality of the devices, increased power demand and a shortened life. Further, small devices have to be designed so that the effect of contamination is minimised, because the small structures of devices cannot be cleaned mechanically or chemically.

The contamination rate, the chemical composition and the physical properties of material deposited on the device surfaces depend on, e.g., outside and indoor air, air flows inside the devices, ambient operation temperatures and the construction materials of the devices. The contamination by chemical compounds is based on the deposition formation by crystallisation and surface reactions. Surface reactions are very harmful, because in a very short time they can change the surface properties (structural and electrostatic) of devices. Therefore, it is important to know the chemical compounds causing the contamination and possible reactions inside the devices. After that, the attachment of depositions can be controlled by choosing the materials for construction such that the interactions between device surfaces and depositions are as weak as possible.

2.2 Fine particles and their deposition mechanisms inside an electronic device

Particles of different sizes come from different sources (see Fig. 2) (Seinfeld & Pandis, 1998). Nucleation-mode particles result from gas-to-particle conversion of different chemical compounds, like sulphuric acid and ammonia. Some nucleation-mode particles are also emitted directly from gasoline engines (Harris & Maricq, 2001). Aitken-mode particles are directly emitted from traffic exhaust, mainly diesel engines. They also result from condensational growth of nucleation-mode particles. Accumulation-mode particles originate from industrial combustion and re-suspension from roadbeds. Some particles also originate from natural sources like sea spraying and cloud processing of particles and vapours. The more polluted the air is, the more accumulation particles there are.

One-micron particles may come from natural sources, re-suspension and combustion, whereas particles of between 1 and 10 microns are mainly mechanically generated; dust, re-suspension, results of industrial processes and sea salt. In developing countries, the main sources are direct emissions from traffic, domestic coal- and biomass-burning and industry.

When an electronic device is used, it is exposed to aerosol particle pollution. Pollution can be transported into the phone by four different mechanisms:

- Convection. Several components heat up during operation. The temperature differences induce convection air flows that can transport aerosol particles into the phone.
- Thermal expansion. Another, possibly important transport mechanism is the thermal expansion of the gas inside the device. If, e.g., the temperature of the gas changes from 25 °C to 85 °C, the volume of the gas changes about 20%. When the air cools down, its volume decreases and new air is imported to the device.
- Mechanically drifting powder material.
- Coarse material (lint, sand and metal particles from keys and the like) is also transported from pocket or bag to the device.

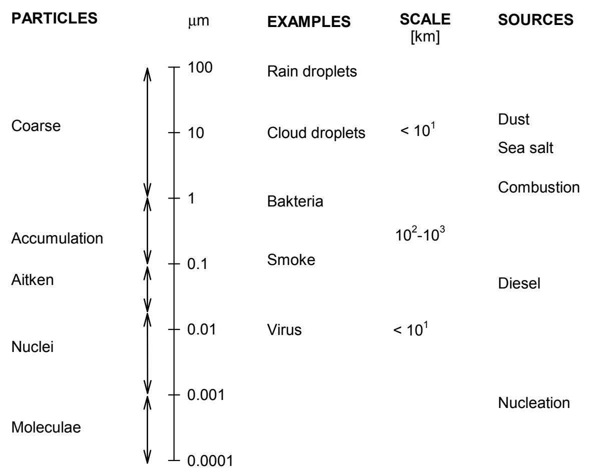

Figure 2. Size scales of aerosol particles. Scale does mean a representative regional transport distance of different particle sizes. It is a combination of typical wind speed and loss mechanisms. For example, nucleation-mode particles coagulate with bigger particles, while coarse particles are deposited rapidly by gravitation. Typical sources and examples of particle types are also shown

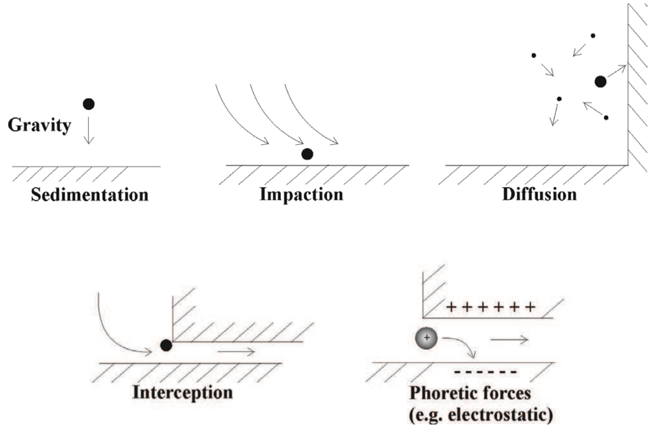

Figure 3. Aerosol particle deposition mechanisms

Once in the device, aerosol particles may be deposited on the internal surfaces of the device. Depending on the aerosol particle size, different mechanisms deposit them in devices. A key aerodynamic property in deposition is the aerodynamic size. For airborne particles, aerodynamic size depends on the particle's shape and density. The aerodynamic size differs from the actual size and accounts for the aerodynamic behaviour of an aerosol. Of all sizes, the accumulation-mode range (0.1–1 µm) penetrates most efficiently through any filter or construction. This is because smaller particles are filtered due to Brownian diffusion, whereas bigger ones are affected by gravitational settling.

The most important deposition mechanisms of airborne particles in electronic devices are sedimentation, impaction, Brownian diffusion, interception and thermophoresis and electrophoresis. These mechanisms are summarised in Fig. 3 and discussed below.

- *Sedimentation.* Sedimentation represents deposition caused by gravity. The chance of particle deposition in the device by sedimentation increases as the particle size, particle density and amount of time (residence time) spent in the airway increase. Deposition by sedimentation is important for particles with an aerodynamic diameter greater than 0.5 µm.
- *Impaction.* When the aerodynamic diameter is larger than 1 µm, particles can be deposited on external device surfaces. The chance of impaction increases as the air velocity, particle size and particle density increase.
- *Brownian Diffusion.* For particles with an aerodynamic diameter less than 1 µm, Brownian diffusion is a major means of deposition in airways where the bulk flow is very low or absent. Deposition by Brownian diffusion is especially important for particles with aerodynamic diameters less than 0.2 µm. Deposition by Brownian diffusion is unimportant for relatively large particles.
- *Interception.* Particle deposition in the air tract can occur when the edge of the particle contacts the airway wall. For elongated particles (e.g., fibres), interception is an important respiratory-tract deposition mechanism. The chance of particle interception increases as the airway diameter becomes smaller.
- *Thermophoretic and electrophoretic forces.* Aerosol particles are often electrically charged. When they are, they can exhibit greater regional deposition than would be expected

from their size, shape and density. The same applies also for strong temperature gradients, which drives particles from warm to cold places.

According to current knowledge, there can be several possibly harmful (for mobile electronic devices) properties of aerosol particles:

- Contamination. Contamination has adverse effects on conductivity. It also makes screens dirty and may damage connectors.
- Contamination combined with chemical effects like corrosion. In this case also relative humidity (RH) and temperature (*T*) are important. In addition to aerosol particles, air flows transfer water vapour and other gases to the phone. Small aerosol particles are often acidic on account of, e.g., sulphuric compounds. Even if the relative humidity is low, some chemical compounds are hygroscopic and may attract water vapour. If air temperature decreases, vapours condense on the internal surfaces because the saturation vapour pressure is a strong function of temperature. If, for example, the temperature of the phone decreases from 30 ^{o}C to 24 ^{o}C at a relative humidity of 70%, condensation takes place.
- The possible effect of aerosol particles on harmful gas compound (e.g., SO_2) deposition. If the surface is covered with aerosol particles, its area can increase greatly, which increases the deposition of gaseous pollutants.

2.3 Effect of water vapour

Water is present in everyday life in many forms, and a cubic metre of typical indoor air contains 5–20 grams of it, depending on temperature and relative humidity. This air-bound humidity is easily transported wherever the air itself goes. If the temperature is dropping, the water stored in air may precipitate and attach to surface structures; in combination with chemical compounds (possibly in particle form), this water may be very corrosive or otherwise harmful. Our studies have focused mainly on particulate matter, but they are closely linked to water studies via estimation of air exchange between the device and its environment, and the polluting potential of particle-bound chemicals.

3. Laboratory studies of particle exposure

In an aim to understand the processes of contamination by particles, the following experimental studies were carried out:

1. Three sets of copper samples were prepared and exposed to ammonium sulphate aerosol particles. The idea was to find a laboratory method to investigate aerosol particle penetration into the phone.
2. The copper samples were investigated by measuring their electrical conductance and using two ion beam methods to determine the surface impurity concentrations.

3.1 Exposure of samples by ammonium sulphate

A polydisperse ammonium sulphate aerosol was generated from an aqueous solution with an atomiser. Droplets from a sprayer were mixed with dry air to solidify the particles. The diluted dry aerosol size distribution was measured using a DMPS where aerosol passed through a charger (bipolar Am-241 neutraliser) and the size distribution of the particles was measured with a differential mobility analyser (DMA) and a condensation particle counter (CPC). The size measurements were done by scanning the voltage of the DMA. The mean particle size in the experiments was about 50 nm, and the total number concentration was on the order of 50,000 cm^{-3}.

The exposures of the copper samples were done in a container (10 cm in diameter and 4 cm high) through which the aerosol was led. The exposure times were 1 day and 4 days for the two pilot samples (case A). A second set of exposures (case B) was done for 4 days and 8 days. For both periods, 2 copper and 2 carbon plates were exposed. Copper plates were investigated with the ERDA method and carbon plates with the RBS method (see section 4.2). In the third experiment set (case C) the samples were prepared by evaporating a 100 nm copper layer on top of a silicon wafer in order to obtain a clean and smooth surface for exposure to ammonium sulphate particles.

3.2 Ion beam analysis

Two different ion beam methods were used for the analysis of the atomic concentrations of different elements on the surfaces of the exposed samples. In both of these methods, the concentration values are based on the detection of the products from scattering reactions between accelerated primary ions and target atoms in the samples under study. The scattering reactions are caused by Coulomb interaction, which is well understood, thus enabling us to obtain accurate results without the use of standard samples.

In the Rutherford backscattering spectrometry (RBS) measurements, 2-MeV He ions were used as incident ions. The RBS method gives accurate and reliable concentration values for impurity atoms, which have higher mass than the main constituents of the sample. This is why carbon backings were used in the RBS measurements. The results indicated clearly the existence of sulphur on the sample surfaces, but no distinct correlation was seen between the exposure time and the sulphur concentration. This may be connected to the observation of large amounts of other impurities in the samples.

In elastic recoil detection (ERD) measurements, 20-MeV iodine ions were used as incident ions. A time-of-flight – energy detector was used to detect simultaneously the energy and the velocity of the recoiled target atoms at an angle of 40^o relative to the incident beam direction. This made it possible to separate different masses of each recoil atom species, and thus to determine at the same time concentrations of all different elements in the samples, from hydrogen up to the heaviest existing atoms. Exposed copper plates and copper films on silicon wafers were analysed with the ERD method.

The results from copper plates indicated the existence of sulphur, among many other impurities, on the sample surfaces, but no clear correlation was seen between the exposure time and the sulphur concentration. This was mainly because of the large amounts of other impurities on the samples; even on the reference samples, which were not exposed to ammonium sulphate particles.

The results from evaporated copper films indicated clear correlation between the aerosol exposure time and impurity concentrations. A large difference between the two samples with longest exposition times can be explained by the position non-homogeneity in the exposition, which was optically visible on the sample surfaces. A surprising result was the relatively large amount of chlorine on the sample surfaces. The sources of chlorine impurities are currently unknown.

4. Air-exchange experiments and modelling

It is difficult to model directly and productively the air flow inside electronic devices without any experimental data. Therefore, we carried out some helium experiments before starting the model development work. The helium method is based simply on use of this inert, small-sized and rather easily analysed noble gas as a tracer in air flow measurements (see, e.g., Hartikainen et al., 1994).

4.1 Helium experiments

In the first part of the experimental study, the phone was placed inside a metal chamber. The helium injection capillary was connected to the right corner of the bottom of the phone, the nitrogen input was connected to the bottom left corner of the metal chamber and the helium exhauster in the upper right corner of the metal chamber (see Fig. 4). First, pure helium was injected inside the phone over 20 seconds, and then the injection capillary was closed. The mixed gas (N_2 + He) flux was measured, and the time constant of total gas flow was calculated from the measured break-through curve (see Fig. 5). The calculated time constant of the total gas flow was 411 seconds.

In the second part of the study, the phone was sealed with elastic gas-tight material (see Fig. 6). Only the selected measuring point was unsealed. The measurement protocol was as follows: 1. Helium was injected inside the phone from point 1 and the overproduction flowed out from point 2. After the phone was filled, both the entry (point 1) and the exit (point 2) channels were closed (see Fig. 6) for 60 seconds. Then the out-flowing gas for the chosen measuring point was measured by helium exhauster. The typical break-through curve is shown in Fig. 7. Local gas flow values were measured from 15 different points (see Table 1).

Results are given as relative gas flow values for every measurement point and as the total time constant. The relative gas flow values were calculated by dividing the measured maximum values (average value of 1.6 to 1.8 minutes) by the maximum value at a reference point.

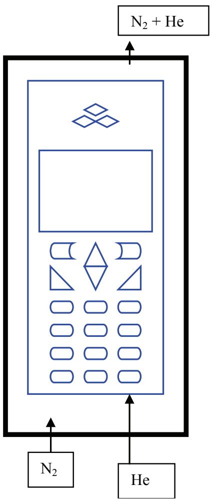

Figure 4. The experimental set-up for the total gas flow through the cover

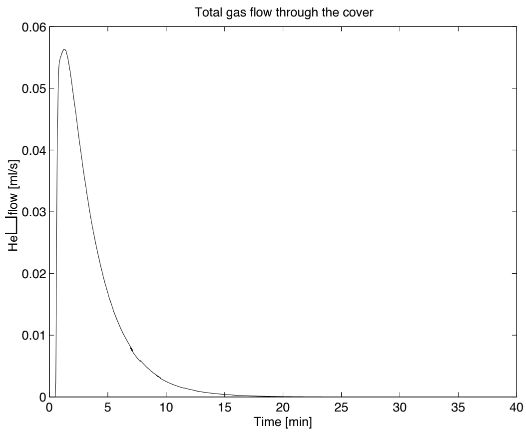

Figure 5. The total gas flow break-through curve

4.2 Analytical helium models

In total, four models (three analytical models and one numerical model, He-fit – see Table 2) were developed to utilise the helium test data from the first experimental set-up. The second helium experiment was fitted by a simple exponential function.

The measured total and void volumes, 70 and 28 ml, respectively, give a porosity value of 0.4. With the macroscopically measured internal surface area, 38,000 ± 10,000 mm², the ratio to void volume gives about 1.4 ± 0.4 mm for mean free distance between internal surfaces.

The simple analytical models consist of two reservoirs, denoted reservoir 1 (free volume of the measurement chamber) and reservoir 2 coupled only to reservoir 1 (internal volume of the mobile phone), the volumes of which are V_1 and V_2, respectively (see Fig. 8). There was constant air flow into and out of reservoir 1. The mean velocity at the outlet was v_{out} and the surface area S_{out}. Between the reservoirs the studied compound is assumed to have an exchange velocity of v_{int}, which is assumed to flow by a surface area of S_{int}. Initially the concentrations in reservoirs 1 and 2 were zero and c_0, respectively.

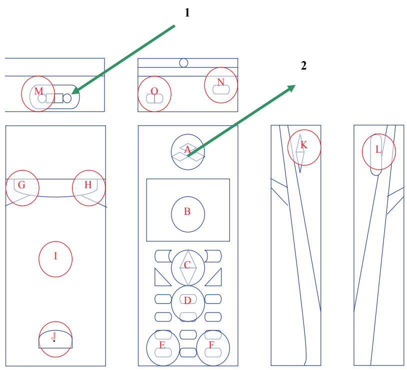

Figure 6. The experimental set-up for the local gas flow through the cover

Measuring point	Relative gas flow value
A	13,700
B	1
C	9,100
D	5,100
E	12,500
F	8,400
G	9,100
H	7,500
I	1
J	8,900
K	11,700
L	8,600
M	10,800
N	10,100
O	73,100

Table 1. The relative gas flow value at point B was equivalent to that at reference point I

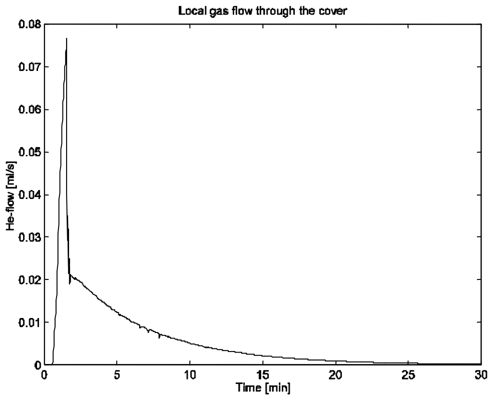

Figure 7. Typical break-through curve for measuring spot H

Name	Description
S1a	Basic analytical model for test case 1
S1b	Well-mixed analytical model for test case 1
S1c	Model S1a without re-flow into mobile phone
S2	Basic analytical model for test case 2
Nfit	Numerical model for test case 1
Nflow	Numerical model for mobile phone flow simulation

Table 2. List of models

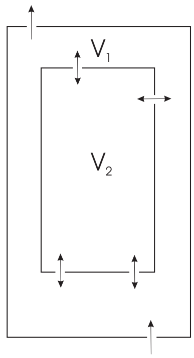

Figure 8. A schematic picture of reservoir volumes used in analytical models

The internal exchange velocity may follow from both molecular diffusion and gas flow, and we assume that the diffusion flux density is a product of diffusivity D_0 (of helium in this case, $6.8 \cdot 10^{-5}$ m^2/s) and gradient of concentration, *c*. A further simplification is that the gradient is approximated by the ratio of mean concentration to characteristic length scale *L*. The internal structure of a mobile phone is quite complicated, causing lengthening of the diffusion path, which is taken account of by correcting the diffusivity via geometric factor *G* (van Brakel & Heertjes, 1974). According to these assumptions, the diffusion flux density (see, e.g., Hinds, 1999), *J*, may be written as

$$J = -D\frac{dc}{dx} \cong -GD_0\frac{c}{L} \tag{1}$$

where $D = GD_0$. If we approximate the mobile phone as a porous medium, the internal surface area, S_{int}, is simply total external surface area *S* multiplied by the porosity, φ. Therefore, the diffusion flux, *q*, is given as

$$q = S_{\mathrm{int}}J \cong -S_{\mathrm{int}}v_{\mathrm{int}}c \tag{2}$$

where $v_{\mathrm{int}} = GD_0/L$.

The characteristic length may be approximated from the dimensions of the mobile phone to be about 20–50 mm. Geometric factor *G* is then a fitting parameter and describes the internal structure of the mobile phone.

First, we developed a model (S1a) for helium test 1 by applying the internal exchange velocity. We can write the following system of linear differential equations for mass balances of the studied compound in both reservoirs:

$$\begin{cases} V_1\dfrac{dc_1}{dt} = -v_{\mathrm{out}}S_{\mathrm{out}}c_1 + v_{\mathrm{int}}S_{\mathrm{int}}\left(c_2 - c_1\right) \\ V_2\dfrac{dc_2}{dt} = -v_{\mathrm{int}}S_{\mathrm{int}}\left(c_2 - c_1\right) \end{cases} \tag{3}$$

The solution with correct initial value is

$$\begin{cases} c_1 = c_0 \dfrac{\lambda_{\text{int}}}{\omega} e^{-\frac{1}{2}(\kappa\lambda_{\text{int}}+\lambda_{\text{int}}+\lambda_{\text{out}})t} \sinh \omega t \\ c_2 = c_0 \left[\cosh \omega t + \dfrac{\kappa\lambda_{\text{int}} - \lambda_{\text{int}} - \lambda_{\text{out}}}{2\omega} \sinh \omega t \right] e^{-\frac{1}{2}(\kappa\lambda_{\text{int}}+\lambda_{\text{int}}+\lambda_{\text{out}})t} \end{cases} \tag{4}$$

where

$$\begin{cases} \lambda_{\text{out}} = \dfrac{v_{\text{out}} S_{\text{out}}}{V_1} \\ \lambda_{\text{int}} = \dfrac{v_{\text{int}} S_{\text{int}}}{V_1} = \dfrac{G D_0 S \varphi}{L V_1} \\ \kappa = \dfrac{V_1}{V_2} \\ \omega^2 = \dfrac{1}{4}\left(\kappa\lambda_{\text{int}} - \lambda_{\text{int}} - \lambda_{\text{out}}\right)^2 + \kappa\lambda_{\text{int}}^2 \end{cases} \tag{5}$$

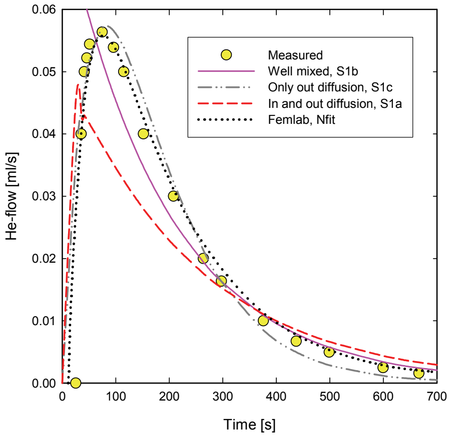

Figure 9. Results of the fittings of the three different analytical models, along with the results of the fitting of the numerical model

Two extreme cases are worth examination: well-mixed (S1b) and a system without return flux into the mobile phone (S1c). The solution for S1b is simply exponential, and S1c has solution

$$\begin{cases} c_1(t) = c_0 \dfrac{\lambda_{\text{int}}}{\lambda_{\text{out}} - \kappa\lambda_{\text{int}}} \left(e^{-\kappa\lambda_{\text{int}} t} - e^{-\kappa\lambda_{\text{out}} t} \right) \\ c_2(t) = c_0 e^{-\kappa\lambda_{\text{int}} t} \end{cases} \tag{6}$$

After fitting the models to one of the experimental data sets, we observed that the simple well-mixed gave the best fit for long times, and the model with internal flux not depending on the external concentration was best at the beginning. All of the model fittings described below are shown in Fig. 9. For internal exchange λ_{int} we obtained the best fit with *a* value of 0.0156 s^{-1}. It is possible to estimate *G* from Eq. 10 (φ = 0.3), which gives *G* = 0.03. Finally, the helium diffusivity in this structure will be $2{\cdot}10^{-6}$ m^2/s.

At the start of the second helium test measurement, there was a peak value (see Fig. 9), but after that the flux decreased clearly exponentially and the fitting gave the value 0.0029 s^{-1} for coefficient λ_{int} .

4.3 Numerical helium models

In addition to analytical models, a phenomena-based (diffusion, fluid flow and thermal conduction) model was developed both for prediction of air-exchange values for this work and to be extended and applied in other systems. The complexity of this model makes only numerical solutions available. FEMLAB® (Comsol AB, 2004a), a commercial interactive environment for modelling and solving problems on the basis of partial differential equations, was chosen as the numerical tool. For particular classes of problems, special modules providing a more comfortable working environment are available. In this work, the Chemical Engineering Module (Comsol AB, 2004b) was applied.

A Navier-Stokes model and Brinkman equation were used to calculate two-dimensional velocity (v_x, v_y) and pressure fields *P* outside and inside the mobile phone, respectively. The Brinkman equation is an extension of the well-known Darcy's law. It is possible to add a force field to Navier-Stokes equations, enabling, for example, modelling of free convection, when the temperature field is given. Conduction-convection was used to calculate temperature in two dimensions.

To model in more detail the transport of helium out of the phone, we developed a numerical model as explained below. The model geometry is shown in Fig. 10. The mobile phone was assumed to be an anisotropic porous system with porosity φ = 0.3. The transport was assumed to occur by diffusion and convection both in the external volume and inside the mobile phone. The air density, ρ , was assumed to be 1.2 kg/m^3, and dynamic viscosity was equal to η = $1.8{\cdot}10^{-5}$ Pa s. The permeability, κ_{B} , needed in the Brinkman equation was fixed at $1.2{\cdot}10^{-5}$ m^2, which is near the value calculated for flow between flat surfaces with a distance of 1.4 mm. The total number of elements was varied from 3,000 to 8,000. Time-dependent simulations were extended from 0 to 1,000 seconds, with logarithmic output times.

The best fit to the experimental data was obtained with *G* = 0.007 in the horizontal direction, and, as assumed, ten times higher in the vertical direction. The modelled out-flow curve is also shown in Fig. 9. The fitted *G* values were then applied in gas flow modelling calculations with the same geometry. The simulated state of the system 7, 52, 139 and 373 seconds after the injection of helium was stopped is shown in Fig. 11.

To estimate the ventilation coefficient (the ratio of the exchanged air volume per unit time to the volume of the system) inside the mobile phone, the same geometry as in diffusion transport calculations was applied. The Brinkman equation in the applied tool is isotropic, and therefore the *G* value was chosen to be the same for both directions.

Finally, we modified the numerical model for cases where temperature differences (due to the heat-producing components) drive the gas transport. This last model was then applied to estimate ventilation coefficients, which may be used in models estimating the long-term contamination of electronic devices. The temperature of the in-flowing gas was set to 25 ºC, the system walls were maintained at a temperature 10 degrees higher and the outer temperature of the battery was kept at 45 °C. These temperature differences caused an inflow of 1 ml/s. Of the total flow into the measuring system, less than 10% was transported via the mobile phone. The simulated velocity fields inside and outside the mobile phone, and temperature both inside and outside, are shown in Fig. 12. From these calculations it can be deduced that a suitable estimate for ventilation coefficient varies from 3 to 10 h^{-1}.

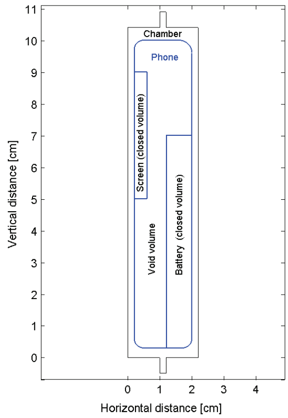

Figure 10. The model geometry for helium and ventilation coefficient calculation is depicted in the figure. Some parts (display and battery) were excluded from the mobile phone – the exclusions were mainly based on results from the second helium experiment

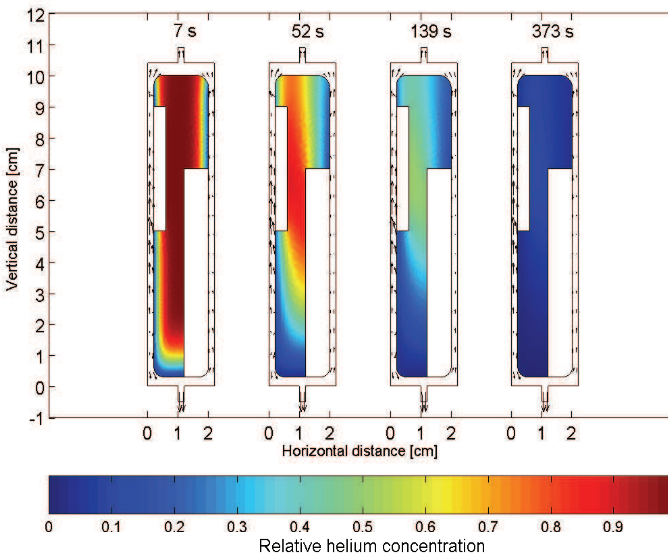

Figure 11. Simulated helium concentration 7, 52,139 and 373 seconds after the beginning of the test. The colour map shows the relative helium concentration inside the phone, and the arrows describe the total flux density of helium outside the phone

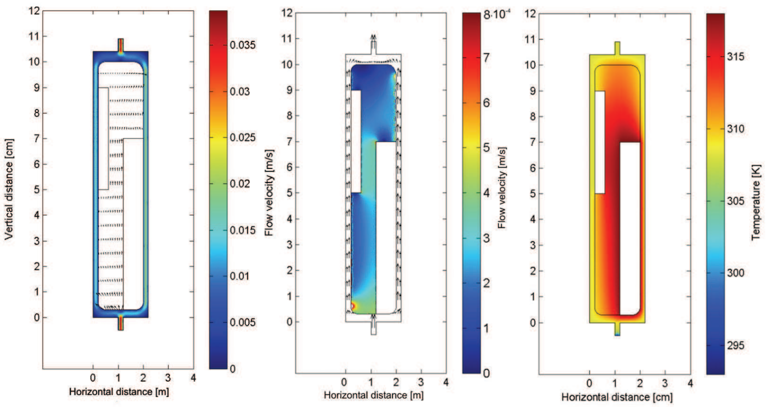

Figure 12. Simulation of flow velocity and temperature inside and outside the phone. The left pane's arrows indicate the velocity inside the phone and the colour-map that outside. In the middle pane, arrows are applied for outside and colours for internal flow velocity. The colour-map (right) shows the temperature distribution both in- and outside the phone

5. Particle penetration models

In this study, we estimated the deposition of harmful aerosol particles in a mobile phone with a multi-step approach, which proceeded from a study of air flows inside a mobile phone (Olin et al., 2006). Next, we generalised an indoor air model to be applied as a contamination model for mobile phones. This model needed some parameter values for both air flow and particle deposition efficiency inside a mobile phone. To have, at least approximate, values of these parameters, we developed a numerical particle transport model, which is described here. The basics and actual application of our contamination model are reviewed only in brief here.

5.1 Governing equations

We developed a coupled particle convection, diffusion and flow velocity model to estimate deposition coefficients of particles of different sizes.

First, we designed a model geometry (see Fig. 13) aimed at describing the inner volume of either end of the mobile phone. The scale of our model may be compared to the matchstick in the same figure. Second, we formed equations for the flow velocity calculations and aerosol particle transport. We applied the Navier-Stokes equations in 2D for flow velocities:

$$\begin{aligned} \frac{\partial v_x}{\partial t} + v_x \frac{\partial v_x}{\partial x} + v_y \frac{\partial v_x}{\partial y} &= -\frac{1}{\rho}\frac{\partial P}{\partial x} + \frac{\mu}{\rho}\left[\frac{\partial^2 v_x}{\partial x^2} + \frac{\partial^2 v_x}{\partial y^2}\right] \\ \frac{\partial v_y}{\partial t} + v_x \frac{\partial v_y}{\partial x} + v_y \frac{\partial v_y}{\partial y} &= -\frac{1}{\rho}\frac{\partial P}{\partial y} + \frac{\mu}{\rho}\left[\frac{\partial^2 v_y}{\partial x^2} + \frac{\partial^2 v_y}{\partial y^2}\right] \end{aligned} \qquad (7)$$

and

$$\frac{\partial v_x}{\partial x_x} + \frac{\partial v_y}{\partial x_y} = 0 \tag{8}$$

The transport of the particles was modelled via the following diffusion-convection equation:

$$\frac{\partial c}{\partial t} + v_x \frac{\partial c}{\partial x} + \left[v_y - v_{\mathrm{TS}}\left(d_{\mathrm{p}}\right) \right] \frac{\partial c}{\partial y} = L\left(d_{\mathrm{p}}\right) \left[\frac{\partial^2 c}{\partial x^2} + \frac{\partial^2 c}{\partial y^2} \right] \tag{9}$$

Diffusion coefficients, L, and terminal settling velocities, v_{TS}, vary quite a lot as a function of particle size (see Table 3). It is important to note that very small particles have high diffusivity while big particles have high terminal velocity, and medium size particles neither diffuse nor drop down clearly in the time scales studied.

5.2 Model implementation

We implemented the governing equations of our particle transport model in the commercial numerical partial differential equation solver FEMLAB® 3.0 together with Chemical Engineering Module (Comsol, 2004a; Comsol, 2004b). The flow velocity (see Fig. 15) was caused by the pressure difference between narrow inlets and outlets (1.0 mm), mainly to create an upward velocity component to compete with the terminal settling velocity.

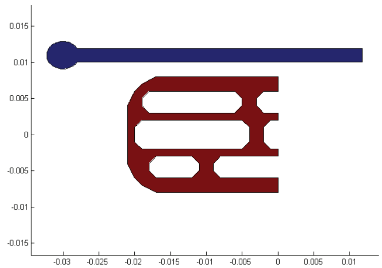

Figure 13. The model geometry applied in our particle transport model and a matchstick (the unit on the axis is the metre)

Diameter (nm)	L (μm²/s)	v_{TS} (μm/s)	<x(1 s)> *diff.* (μm)	<x(100 s)> *diff.* (μm)	100 s x v_{TS} (μm)
10	54,000	0.07	330	3,300	7
30	5,800	0.2	110	1,100	20
100	690	0.88	37	370	88
300	130	4.4	16	160	440
1,000	27	35	7.4	74	3,500
3,000	7.8	270	4.0	40	27,000

Table 3. Diffusion coefficients and terminal settling velocities for some particle diameters (Hinds, 1999). Particles are assumed to be spherical and their density 1,000 kg/m³. In addition, the mean distances from diffusion in 1 and 100 seconds is calculated; for comparison, distance travelled by terminal settling in 100 seconds is given also. Particles with a diameter of 100–300 nm are neither diffusing nor settling in this time

The mesh was made denser at all surfaces to enable the calculation of particle diffusion flux to them (see Fig. 14). Particles were assumed to have zero concentration at all solid surfaces, which creates sharp gradients. All told, 20,576 mesh elements, of which 2,000 were surface elements, were created for most calculations, giving about 200,000 degrees of freedom. In some cases (e.g., with large particles, when gravitational settling was dominating), more elements were needed, but with the applied computer (0.5 GB memory) this was not possible.

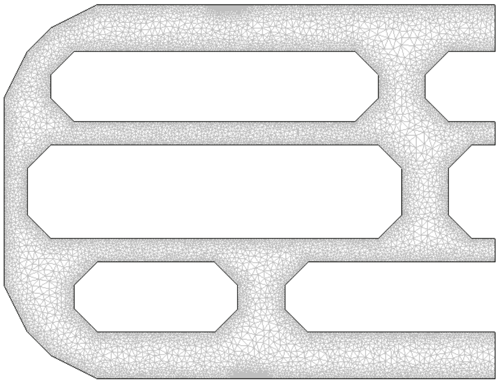

Figure 14. The applied mesh

5.3 Model applications

We applied the model in calculation of important parameter values needed in the simplified contamination model. In total, seven different cases (from pure diffusion to maximum inlet flow velocity of 3.0 mm/s) were calculated for particle diameters 30, 100, 300, 1,000 and 3,000 nanometres (particle density 1,000 kg/m^3). The applied pressure differences, inlet velocities and corresponding ventilation coefficients in our simplified contamination model are shown in Table 4.

All told, 34 test-case calculations were made to include all flow velocity cases and all studied particle diameters. In nine test cases, our model did not converge well. The test cases are named by particle diameter in nanometres and by the flow velocity code, and all test-case names start with 'D'; for example, D100_AA represents the 100-nanometre particles in case AA. In figures 17 and 18, relative concentration inside the system studied is shown for 12 selected test cases.

Case	ΔP (μPa)	v (mm/s)	l (h^{-1})
0	0	0 *	
AAA	9,2	0.01	0.23
AA	27,6	0.03	0.69
A	92	0.1	2.3
B	276	0.3	6.9
C	920	1.0	23
D	2 760	3.0	69

* Diffusion only

Table 4. Case numbers, pressure difference ΔP, inlet velocity v and ventilation coefficient l

In the present work, we were mainly interested in the calculated values of deposition rates, *a*, which are tabulated in Table 5 and shown in Fig. 16. There was a clear minimum in *a* values for particle sizes at around 100 to 300 nm, which means that particles of that size are neither diffused on surfaces nor settled by gravitation on horizontal surfaces. These effects or the lack of them can be seen readily in relative concentration (figures 17 and 18).

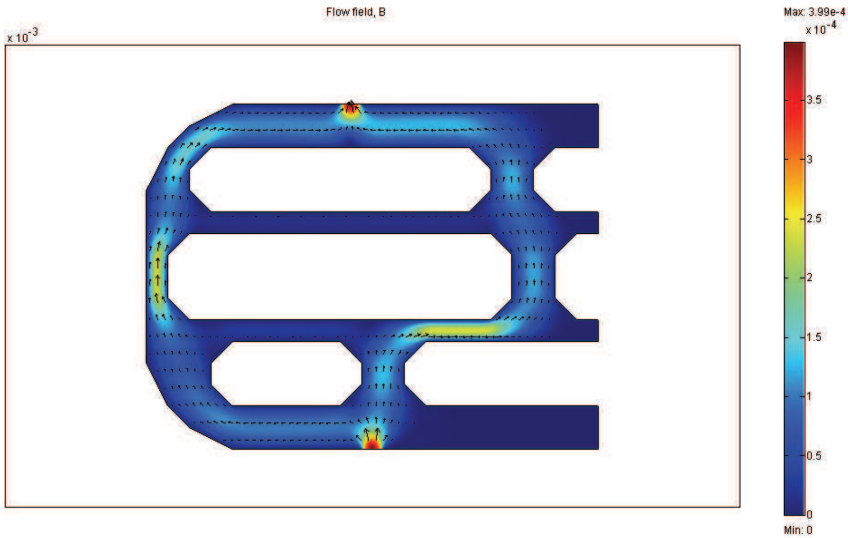

Figure 15. The calculated velocity field for case B. All other cases were similar, except, of course, that the velocity scale varied. The geometry was intentionally created such that both routes from inlet to outlet are in use

d_p (nm)	0	AAA	AA	A	B	C	D
10	645	628	583	474	299	368	412
30	70	52	40	39	44	52	84
100	15	4.7	5.3	5.9	9.0	19	39
300	55	9.2	7.2	6.8	7.3	14	35
1,000	nr	nr	nr	63	54	49	75
3,000	nr	Nr	nr	nr	nr	363	409

Table 5. Calculated deposition rate *a* (in h^{-1}) for test cases as a function of particle diameter (nr = the model didn't converge)

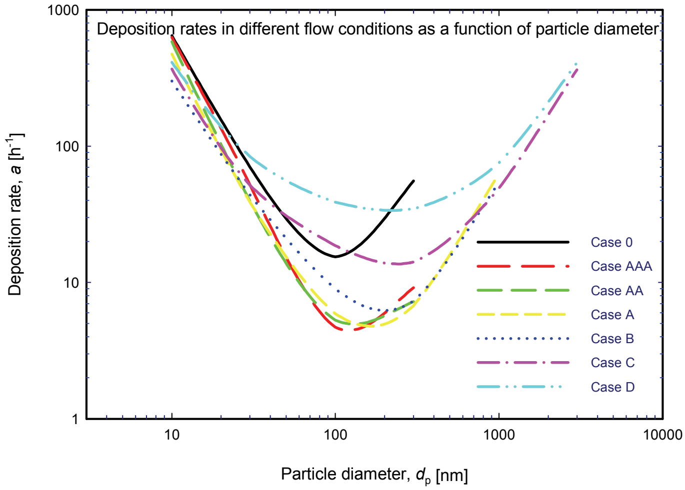

Figure 16. Deposition rate as a function of particle diameter in different cases. There is a clear minimum, which is lowest in the cases with lowest flow velocity

5.4 Simplified contamination model for particle accumulation estimates

In order to calculate long-term contamination of mobile electronic devices, we modified our indoor model (Raunemaa et al., 1989) to create a phone contamination model to suit these new conditions. Below, the contamination model is briefly reviewed.
Deposition is characterised by a set of equations (see, e.g., Raunemaa et al., 1989):

$$\frac{dI(d_p)}{dt} = l \cdot s \cdot (d_p) \cdot O(d_p) - \left[l + a(d_p)\right] I(d_p) + r(d_p) \cdot B(d_p) + Q(d_p) + D(d_p) \tag{10}$$

$$\frac{dB(d_p)}{dt} = \frac{V}{A}\left[a(d_p) \cdot I(d_p) - r(d_p) \cdot B(d_p)\right] \tag{11}$$

$$\frac{dO(d_p)}{dt} = f(t, d_p) \tag{12}$$

A very important part of this modelling approach is the estimation of necessary parameters: air-exchange coefficient l, penetration coefficient s and deposition rate a. We were not able to deduce them from some earlier studies. Therefore, the main application of our particle transport model was to find values for these parameters, in mobile phone applications. Source term Q includes many different phenomena, which are beyond the scope of this presentation.

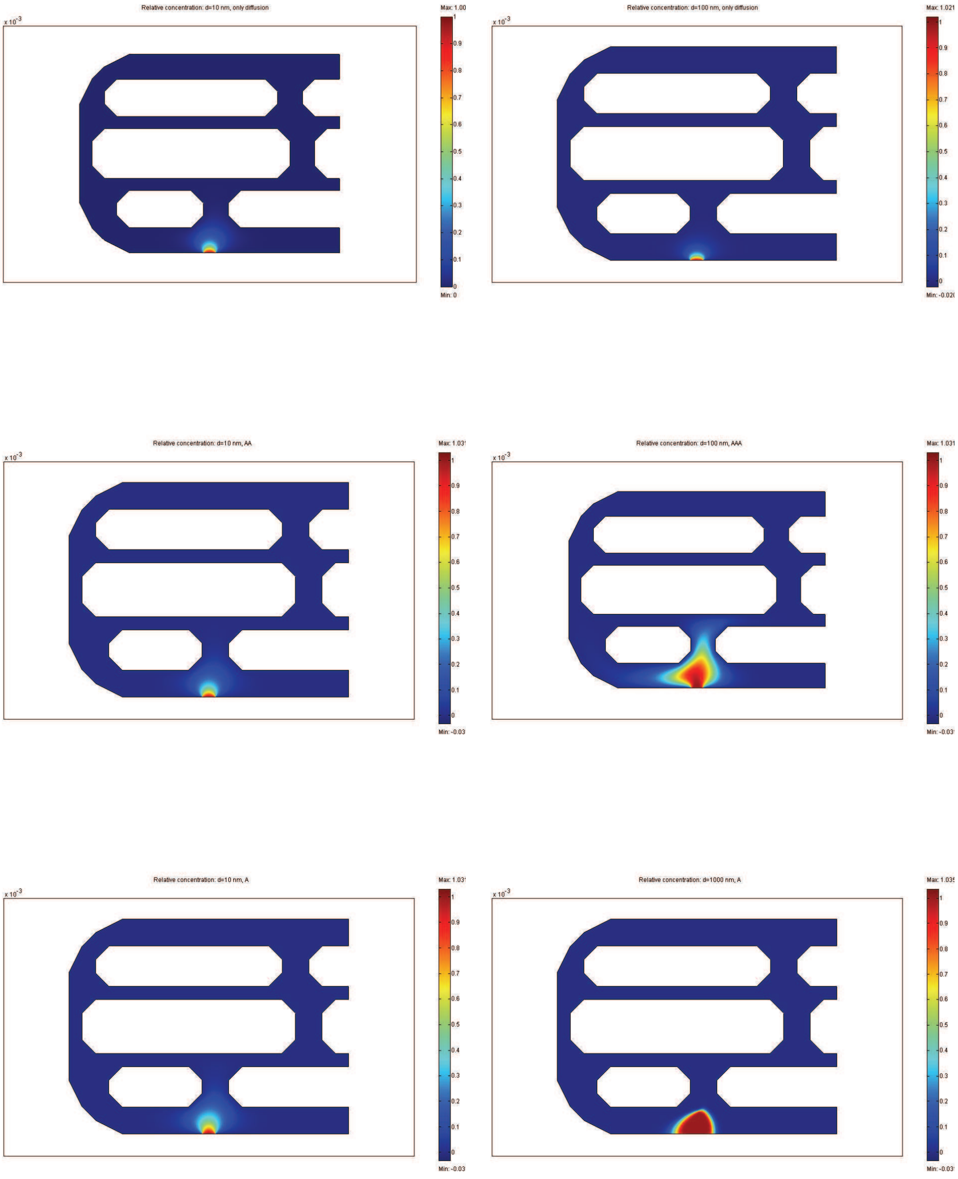

Figure 17. Test cases D10_0, D10_AA, D10_A, D100_0, D100_AAA and D1000_A. In these cases either diffusion or gravitational settling limits the particles' penetration into the system

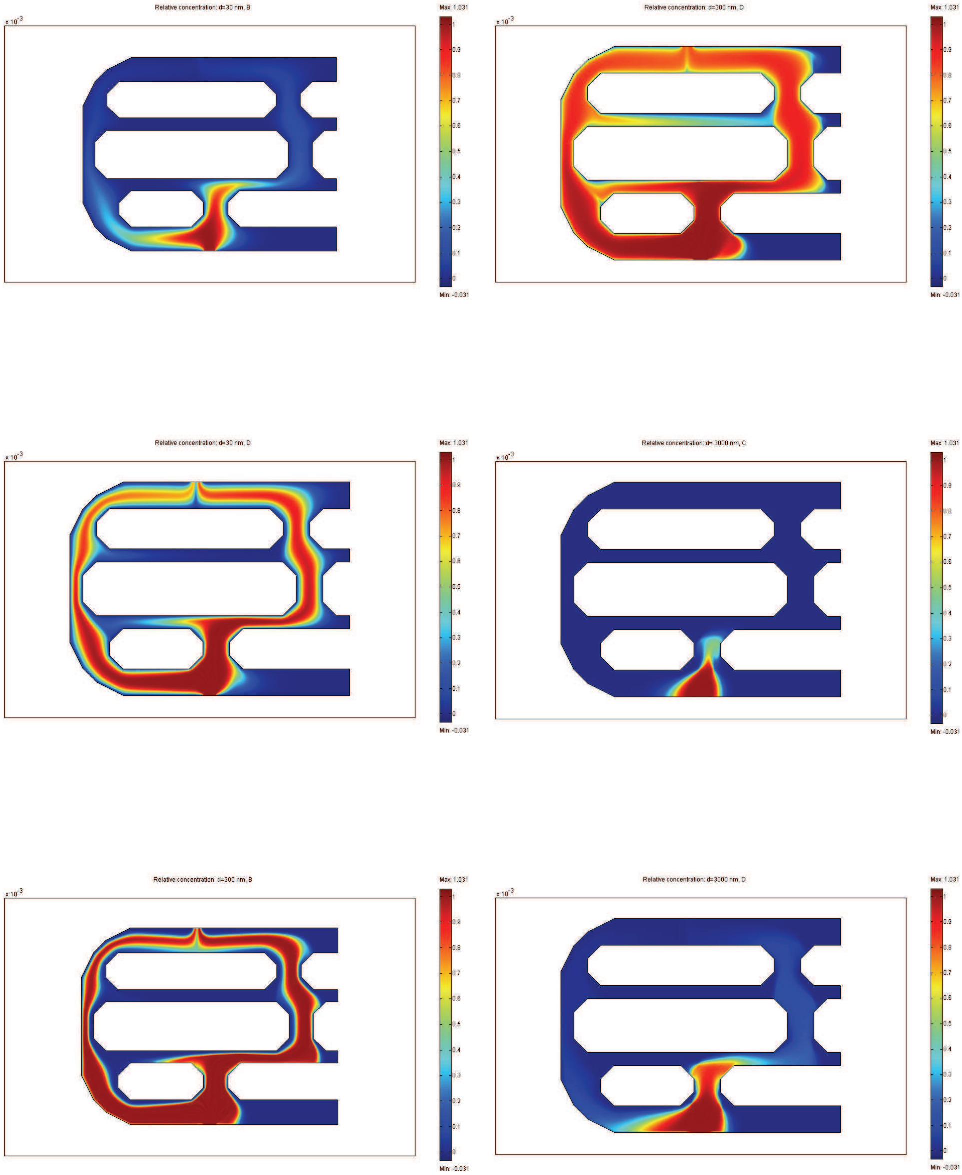

Figure 18. Test cases D30_B, D30_D, D300_B, D300_D, D3000_C and D3000_D (from top to bottom). In these test cases, the particles may even go via the whole system. This is especially clear for particles of size class 300 nm

Diffusion is given by Fick's first law:

$$D(d_p) = L(d_p)\frac{O(d_p) - I(d_p)}{dx}\frac{A_r}{V} \tag{13}$$

If the following assumptions are made:

$r(d_p) = 0$ No re-emission (i.e., particles stay on surface once deposited)

$Q(d_p) = 0$ No sources inside the phone

$f(t, d_p) = 0$ Annual average concentration is used

$I(0, d_p) = 0$ Initial indoor concentration of zero

$B(0, d_p) = 0$ Initial accumulated material of zero

one gets for the indoor concentration

$$I(d_p) = \frac{v_1}{v_2}\left(1 - e^{-v_2 t}\right) \tag{14}$$

and for surface deposition

$$B(d_p) = \frac{v_1 v_3}{v_2}\left[t - \frac{1}{v_2}\left(1 - e^{-v_2 t}\right)\right] \tag{15}$$

where

$$v_1 = \left[ls(d_p) + \frac{L(d_p)A_r}{dx \cdot V}\right]O(d_p), \tag{16}$$

$$v_2 = l + a(d_p) + \frac{L(d_p)A_r}{dx \cdot V} \tag{17}$$

and

$$v_3 = \frac{a(d_p)V}{A} \tag{18}$$

5.4 Application of simplified contamination model

Based on helium and laboratory measurements, and FEMLAB® results, a rough model was created. It was used for two different environments, New Delhi and Helsinki (Laakso et al., 2006). All calculations were done for two characteristic user types: a basic user and a heavy user. The results show for seven years of use that in New Delhi approximately 30% of the inner surfaces of the phone can be covered by aerosol particles in the case of a heavy user. For a basic user, the coverage was less than 5%. In Helsinki, the corresponding figures were about 4% and less than 1%. It was also found that the accumulation-mode particles were responsible for most of the coverage, on account of their large surface, relatively high concentrations and capability to penetrate the phone deeply. However, it should be kept in mind that the coverage inside the phone is not uniform. It depends a great deal on the flow fields and apertures. When the different use situations were compared, it was found that most of the contamination came about in the case of a heavy user from the call, whereas in the case of the basic user the contamination was due to residual air remaining in the phone after the call.

6. Conclusions and discussion

Our first problem was how to study the air exchange of a small electronic device. The helium method was one option among others, and results from these studies are collected in this article. The helium experiments were completed successfully, even though the method was being applied for only the first time with electronic devices. When the experiments started, it was not very clear which strengths and weaknesses the method has. The first observation was that the results had no real meaning without extensive modelling, which enables conclusions to be drawn from experimental results.

During the modelling work it was observed that it is important to include all three basic transport phenomena (mass, heat and momentum) and their couplings (via transport parameters) in the model calculations. A few degrees of temperature difference may cause observable gas velocities, which often transport gases more rapidly than diffusion. Therefore, the application of some computational tool enabling the estimation of these effects even in complicated geometrical structures is highly recommendable.

On the basis of these steps, we were able to calculate air-exchange coefficient values for a specific mobile phone model – the mobile in use, in vertical orientation and in warm conditions. The uncertainties are high, and small variations in the conditions (heat source and temperature field) and assumed structure (the gas-permeability of the cover and internal parts) of the mobile phone increase the variation to 0.5–50 1/h. The uncertainties may be rendered smaller via application of a more detailed geometric model and knowledge of heat sources inside the mobile phone. Results from this study can be used in developing requirements, corresponding test cases and design guides for electronic devices.

Our second problem was to calculate aerosol particle deposition rates for a portable electronic device. The result was that very small and big particles do not easily penetrate the structure deeply, because of diffusion on surfaces and gravitational settling, respectively. Medium-sized particles (of a diameter between 50 and 500 nm), by contrast, penetrate the inner structures and may even pass through the whole apparatus. In the figures, relative particle concentrations for 100- and 1,000-nm particle diameters in the same flow conditions are shown.

In future, it will be desirable to control the contamination of electrical and electronic devices even better than is done today. Because direct experimental measurements in electronic devices are complicated as a result of the detailed and heterogeneous structure of the devices, the role of different modelling and simulation methods becomes more significant. Various molecular modelling techniques have been widely used to estimate chemical reactions among single atoms or small molecules, properties of solid materials and adsorption behaviour of small molecules on solid surfaces (Leach, 2001). We have applied molecular modelling techniques in contamination studies of heat-transfer surfaces (Puhakka et al., 2007). The main advance in molecular modelling was found in defining reaction pathways that may not be defined from process measurements and fouling resistance curves.

In particular, *ab initio* methods are very convenient, because no experimental parameters are needed. There are two main categories: the Hartree-Fock methods and density functional methods (Leach, 2001). The effectiveness of molecular techniques becomes more important when new construction materials like chemical and physical vapour deposition (CVD and PVD) coatings for microelectronics are designed and experimental measurements are not available. Solid techniques make it possible to perform estimations of coating properties in prevention of contamination by means of modelling techniques.
Our main conclusion is that numerical calculations of the particle transport inside electronic devices yield very valuable information about the processes, and, simultaneously, they offer a way to approximate certain important parameters in more practical contamination models. We recommend further modelling with different and perhaps a three-dimensional geometry. The model is applicable to all kinds of small apparatus. Results from this study can be used in developing requirements, corresponding test cases and design guides for electronic devices.

7. Nomenclature

Definitions	
Nucleation mode	particles having diameter between 0 and 30 nm
Aitken mode	particles having diameter between 30 and 80 nm
Accumulation mode	particles having diameter between 80 and 1,000 nm
RBS	Rutherford backscattering spectrometry
ERDA	Elastic Recoil Detection Analysis
Helium and phone	
c	concentration [kg m^{-3}]
D	diffusivity [m^2 s^{-1}]
d, d_p	particle diameter [nm, µm, m]
G	geometric factor, which corrects the diffusivity to take account of the longer diffusion path and the form of pores
J	flux density [kg s^{-1} m^{-2}]
l	air exchange coefficient [h^{-1}]
L	characteristic length scale [m]
q	flux [kg s^{-1}]
S	surface area [m^2]
v	velocity [m s^{-1}]
V	volume [m^3]
v_{TS}	gravitational settling velocity for particles [m s^{-1}]
κ	ratio of volumes
λ	exchange coefficients [h^{-1} or s^{-1}]
φ	porosity, fraction of void space in porous system
Phone contamination	
A	internal area of the phone [cm^2]
$a(d_p)$	deposition rate [h^{-1}]
A_r	area of the chinks [cm^2]
$B(d_p)$	surface accumulation [cm^{-2}]
$D(d_p)$	diffusion in -transport
dx	diffusion distance [cm]

$f(t,d_p)$	outdoor concentration change [cm^{-3} h^{-1}]
$I(d_p)$	indoor concentration [cm^{-3}]
l	air exchange rate [h^{-1}]
$L(d_p)$	particle diffusion coefficient [cm^2 h^{-1}]
$O(d_p)$	outdoor concentration [cm^{-3}]
P	pressure [Pa]
$Q(d_p)$	the indoor source rate [cm^{-3} h^{-1}]
$r(d_p)$	re-emission rate [$cm^{-1}h^{-1}$]
$s(d_p)$	penetration coefficient []
V	void volume of the phone [cm^3]
μ	dynamic viscosity [Pa s]
ρ	density [kg m^{-3}]

8. References

Baldasano, J.M.; Valera, E. & Jimenez, P. (2003). Air quality data from large cities. *Air Quality Data from Large Cities*, Vol. 307, 141-165

Comsol AB (2004b). *FEMLAB Chemical Engineering Module User's Guide, Version 3.0*

Comsol AB (2004a). *FEMLAB User's Guide and Introduction, Version 3.0*

Hannula, J. (2001). Statistical approach for determination of usage environments, Master's Thesis, University of Helsinki, Helsinki

Harris, S.J. & Maricq, M.M. (2001). Signature size distributions for diesel and gasoline engine exhaust particulate matter. *Journal of Aerosol Science*, Vol. 32, 749-776

Hartikainen, K.; Väätäinen, K.; Hautojärvi, A. & Timonen, J. (1994). Further development and studies of gas methods in matrix diffusion. *MRS*, Vol. 333, 821-826

Hinds, W.C. (1999). *Aerosol Technology*, Wiley, New York

Laakso, L.; Olin, M.; Hämeri, K.; Kulmala, M.; Hannula, J.; Galkin, T. & Väkeväinen, K. (2004). Deposition of aerosol particles in portable electronic devices, Nokia-internal report

Laakso, L.; Koponen, I.K.; Mönkkönen, P.; Kulmala, M.; Kerminen, V.-M.; Wehner, B.; Wiedensohler, A.; Wu, Z. & Hu, M. (2006). Aerosol particles in the developing world: A comparison between New Delhi in India and Beijing in China. *Water, Air and Soil Pollution*, 1-16, DOI 10.1007/s11270-005-9018-5

Leach, A.R. (2001). *Molecular Modelling: Principles and Applications*, 2nd ed., Pearson Education Limited, Essex

Ojala K. & Väkeväinen K. (2001). Data logger device for usage environment of mobile phones, IEST 47th Annual Technical Meeting, Phoenix

Olin M.; Laakso L.; Hannula J.; Galkin T.; Väkeväinen K. & Hartikainen K. (2006). Experimental and theoretical studies on air exchange of portable devices, Comsol Conference Copenhagen

Puhakka, E.; Riihimäki, M. & Keiski, R.L. (2007). Molecular modeling approach on fouling of the plate heat exchanger: Titanium hydroxyls, silanols, and sulphates on TiO_2 surfaces. *Heat Transfer Engineering,* Vol. 28, No. 3, 248-254

Raunemaa, T.; Kulmala, M.; Saari, H.; Olin, M. & Kulmala, M.H. (1989). Indoor air aerosol model: Transport indoors and deposition of fine and coarse particles. *Aerosol Science and Technology*, Vol. 11, 11-25

Roberge, P.R.; Klassen, R.D. & Haberecht, P.W. (2002). Atmospheric corrosivity modeling – a review. *Materials & Design*, Vol. 23, 321-330

Scholorling, M. (2000). At Sixth International Conference on Urban Transport and the Environment for the 21st Century, Cambridge, 26-28 July

Seinfeld, J.H. & Pandis, S.N. (1998). *Atmospheric Chemistry and Physics: From Air Pollution to Climate Change*, Wiley, New York

van Brakel, J. & Heertjes, P.M. (1974). Analysis of diffusion in macroporous media in terms of a porosity, a tortuosity and a constrictivity factor. *International Journal of Heat Mass Transfer*, Vol. 17, 1093-1103

Väkeväinen K.; Hannula, J. & Ojala, K. (2001). Determination of usage environment of mobile phones, IEST 47th Annual Technical Meeting, Phoenix

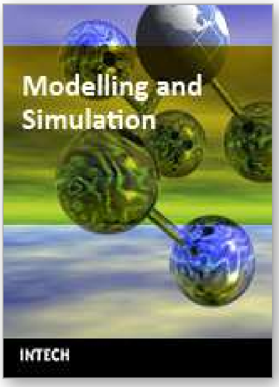

Modelling and Simulation
Edited by Giuseppe Petrone and Giuliano Cammarata

ISBN 978-3-902613-25-7
Hard cover, 688 pages
Publisher I-Tech Education and Publishing
Published online 01, June, 2008
Published in print edition June, 2008

This book collects original and innovative research studies concerning modeling and simulation of physical systems in a very wide range of applications, encompassing micro-electro-mechanical systems, measurement instrumentations, catalytic reactors, biomechanical applications, biological and chemical sensors, magnetosensitive materials, silicon photonic devices, electronic devices, optical fibers, electro-microfluidic systems, composite materials, fuel cells, indoor air-conditioning systems, active magnetic levitation systems and more. Some of the most recent numerical techniques, as well as some of the software among the most accurate and sophisticated in treating complex systems, are applied in order to exhaustively contribute in knowledge advances.

How to reference
In order to correctly reference this scholarly work, feel free to copy and paste the following:

Markus Olin, Lauri Laakso, Jukka Hannula, Timo Galkin, Kyösti Väkeväinen, Kari Hartikainen and Eini Puhakka (2008). New Methods to Model and Simulate Both Air Exchange and Particle Contamination of Portable Devices, Modelling and Simulation, Giuseppe Petrone and Giuliano Cammarata (Ed.), ISBN: 978-3-902613-25-7, InTech, Available from: http://www.intechopen.com/books/modelling_and_simulation/new_methods_to_model_and_simulate_both_air_exchange_and_particle_contamination_of_portable_devices

InTech Europe
University Campus STeP Ri
Slavka Krautzeka 83/A
51000 Rijeka, Croatia
Phone: +385 (51) 770 447
Fax: +385 (51) 686 166
www.intechopen.com

InTech China
Unit 405, Office Block, Hotel Equatorial Shanghai
No.65, Yan An Road (West), Shanghai, 200040, China
中国上海市延安西路65号上海国际贵都大饭店办公楼405单元
Phone: +86-21-62489820
Fax: +86-21-62489821